Atomic-scale electrochemistry on the surface of a manganite by scanning tunneling microscopy

ARTICLE *in* APPLIED PHYSICS LETTERS · APRIL 2015

Impact Factor: 3.3 · DOI: 10.1063/1.4917299

5 AUTHORS, INCLUDING:

Alexander Tselev
University of Tennessee
137 PUBLICATIONS **1,533** CITATIONS
SEE PROFILE

Anthony Gianfrancesco
University of Tennessee
12 PUBLICATIONS **25** CITATIONS
SEE PROFILE

Arthur P Baddorf
Oak Ridge National Laboratory
170 PUBLICATIONS **3,377** CITATIONS
SEE PROFILE

Sergei V Kalinin
Oak Ridge National Laboratory
623 PUBLICATIONS **11,091** CITATIONS
SEE PROFILE

Accepted in Applied Physics Letters

Atomic-scale electrochemistry on the surface of a manganite by scanning tunneling microscopy

Rama K. Vasudevan[1,2,*], Alexander Tselev[1,2], Anthony G. Gianfrancesco[3], Arthur P. Baddorf[1,2] and Sergei V. Kalinin[1,2,3]

[1]Center for Nanophase Materials Sciences, Oak Ridge National Laboratory, Oak Ridge TN 37831, USA

[2]ORNL Institute for Functional Imaging of Materials, Oak Ridge National Laboratory, Oak Ridge TN 37831, USA

[3]UT/ORNL Bredesen Center, University of Tennessee, Knoxville, TN

Abstract

The doped manganese oxides (manganites) have been widely studied for their colossal magnetoresistive effects, for potential applications in oxide spintronics, electroforming in resistive switching devices, and are materials of choice as cathodes in modern solid oxide fuel cells. However, little experimental knowledge of the dynamics of the surfaces of perovskite manganites at the atomic scale exists. Here, through *in-situ* scanning tunneling microscopy (STM), we demonstrate atomic resolution on samples of $La_{0.625}Ca_{0.375}MnO_3$ grown on (001) $SrTiO_3$ by pulsed laser deposition. Furthermore, by applying triangular DC waveforms of increasing amplitude to the STM tip, and measuring the tunneling current, we demonstrate the ability to both perform and monitor surface electrochemical processes at the atomic level, including formation of oxygen vacancies, and removal and deposition of individual atomic units or clusters. Our work paves the way for better understanding of surface oxygen reactions in these systems.

Keywords: scanning tunneling microscopy, manganites, oxygen vacancies, atomic manipulation

*rvv@ornl.gov

Strong electronic correlations in oxides underpin the physics of an important branch of condensed matter physics, the most widely celebrated being high temperature superconductors[1] and the related Mott insulators[2]. One of the most widely explored classes of these materials are mixed-valence manganites[3], in which the strong electronic correlations are coupled with additional degrees of lattice and charge freedom[4] results in phenomena such as coexistence of metallic and insulating phases[5,6], colossal magnetoresistance, and charge ordering producing rich phase diagrams that have attracted attention for the best part of the last two decades. Owing to its high conductivity and low thermal mismatch with Zr-based solid electrolytes, the manganite series $La_xSr_{1-x}MnO_3$ has been used as the cathode material in solid oxide fuel cells[7], where oxygen vacancies and molecular oxygen react and reduce to oxygen ions. Due to their high electrochemical activity, doped manganite thin films have also been explored for memory applications[8] based upon a resistive switching mechanism, wherein the resistance state may influenced by electrochemical migration of oxygen vacancies through application of electric fields[9].

From a fundamental perspective the properties of manganite surfaces are heavily dependent on the terminations involved[10], the type of the surface reconstruction[11] and the local chemical disorder[12]. A factor crucial to this inherent physical complexity is the competition between the electron localization and delocalization in the crystal lattice: localization stems from the Jahn-Teller distortion of the octahedral unit cell, which can couple cooperatively with adjacent cells to minimize lattice strain and result in percolation of a charge-ordered insulating phase[13], whereas delocalization leads to ferromagnetic behaviour but suppresses electron-phonon coupling. Importantly, due to the wide range of phase coexistence[5,14] in these systems, properties such as transition temperatures, magnetoresistance and conductivity have been seen to be highly

dependent on strain[15-17], suggesting thin film epitaxial growth techniques can be used to both study and tune the properties at the surface. Moreover, the properties of the manganites are known to be very sensitive to the oxygen stoichiometry. For example, the charge ordering phase may transition from commensurate (Mn^{3+}/Mn^{4+} = 1) to incommensurate as the oxygen stoichiometry changes from O_3 to $O_{3-\delta}$ [18], while epitaxial manganite thin films annealed in oxygen are known to show improved transport properties[19].

A more detailed understanding of all physical and electrochemical phenomena inherent in these systems would strongly benefit from in-depth atomic-scale studies, for example using scanning tunnelling microscopy (STM). Local probes such as STM can provide more insight into the chemical aspects, such as the surface oxygen stoichiometry, as well as the physical aspects. For materials that cannot be cleaved, one approach is to grow oxide thin films and transfer them *in-situ*, without breaking vacuum into an STM chamber for imaging and/or other surface analysis. Following this approach, Fuchigami et al.[11] grew films of $La_{0.625}Ca_{0.375}MnO_3$ and imaged reconstructions of oxygen on the surface which could be changed by annealing, resulting in different electronic properties, while Ma et al.[20] successfully imaged localized holes in $(La_{5/8-0.3}Pr_{0.3})Ca_{3/8}MnO_3$.

Here, we extend the concept of *in-situ* studies of the manganese oxide films by using the STM tip as a direct single atom electrochemical probe, and show manipulation on the atomic scale on the surface with the STM tip. Such experiments are an example of atomic manipulation on the surface of a manganite at the atomic level, paving the way for better understanding of surface oxygen reactions in these systems. Films of $La_{0.625}Ca_{0.375}MnO_3$ (LCMO) were grown using pulsed laser deposition on TiO_2-terminated (100) $SrTiO_3$ (STO) substrates at a substrate temperature of 750°C in oxygen partial pressure of 50 mTorr, with rapid cooling (at deposition

pressure) at 150°C/min immediately after deposition to minimize oxygen adatom adsorption. Deposition was stopped after 25 unit cells were complete, and cooling below 400°C was carried out in vacuum. Additional details about the growth, surface structure and chemical characterization are reported elsewhere.[21] LCMO grows in a layer-by-layer growth mode[11,20]; the film growth here was stopped after 24 unit cells.

Immediately after the growth, the sample was cooled and transferred to an STM chamber (without breaking vacuum) for imaging on an Omicron STM. The STM tips used were mechanically cut Pt/Ir wire acquired from Agilent and subsequently heated in UHV by passing a large (~5A) current through the tip for ~10s for cleaning prior to use. All images were taken at room temperature with the tip biased and the sample grounded. Typical STM scanning parameters were V_{tip} = -1.8V, I_{tip} = 60pA. Imaging with positive (negative) bias with this setup probes the filled (empty) electronic states. We note that continuous scanning with a positive tip bias was not achievable due to tip-sample instability, presumably associated with pick-up of surface atoms, which we use to our advantage (below).

A typical larger scale STM image of the surface, taken across a step edge, is shown in Fig. 1(a), and shows that much of the surface is covered with small islands about 5nm in width. A line profile taken across three of these islands, indicated by the solid green line in Fig. 1(a), is shown in Fig. 1(b), and indicates heights between 200-300pm, or just over half a unit cell, i.e. it appears the film is mixed terminated. A close-up view of several islands and the film is shown in the STM image in Fig. 1(c). This image reveals that we can obtain atomic resolution on the islands, but the other termination appears disordered. An expanded view of the dashed box in Fig. 1(c) is shown in the inset in the figure, showing that the lattice on the islands consists of a rotated square pattern. An FFT of this island is also shown inset, and indicates a periodicity of

~0.55nm. In other words, the islands are reconstructed into a $(\sqrt{2} \times \sqrt{2})R45°$ structure.. The surface terminations of our LCMO films have been studied in detail using STM and angle-resolved x-ray photoemission spectroscopy, and have been reported and discussed elsewhere.[21] The results from that study allow identification of the islands in this film as (La,Ca)O, and the other termination as MnO_2. Additionally, it should be noted that we are imaging the oxygen in the (La,Ca)O islands. A schematic for the non-relieved (La,Ca)O-terminated state of the LCMO film is shown in Fig. 1(d) with the oxygen atoms of the (La,Ca)O and MnO_2 terminations shown in purple and red, respectively.

Having explored the surface structure, we attempted atomic manipulation with the STM tip. In Fig. 2(a), a disordered area of the surface is seen in the STM image, with a small island in the lower left (inset, expanded view). The tip was placed at the red circle in Fig. 2(a) and held at +2.5V for 8s, and the same region was scanned again to observe the effects of the bias application. The STM image after bias application is shown in Fig. 2(b), and clearly indicates that the disordered feature marked by 'X' in Fig. 2(a) has been removed or displaced as a result of the bias application, revealing more of the underlying surface.

Having confirmed the possibility to modify the surface by application of positive bias, we employed somewhat more sophisticated waveforms to determine the onset bias for these electrochemical reactions. We use a sawtooth type waveform, consisting of triangular DC waveform segments of increasing magnitude, applied to the STM tip whilst the Z-feedback is turned off. The basic premise of the measurement is to determine the activation bias for any generic electrochemical reaction occurring under the tip, which will correlate to the lowest bias at which the I-V loops begin to show a non-negligible hysteresis[22]. These types of measurements were initially carried out mesoscopically with an atomic force microscopy tip for Ca-doped

$BiFeO_3$[22], and here we apply the same technique to the atomic scale with STM. The current is simultaneously monitored upon application of this waveform. Each cycle of the waveform contains a forward and reverse branch, and is applied slowly (~a few s) to monitor reaction kinetics *in-situ*[23]. If there are no changes in atomic configuration, then the forward and reverse curves should coincide. But once there are such changes, this will manifest as hysteresis (or current spikes), and therefore the onset of hysteresis or a sudden current increase or decrease is the sign of the onset of an electrochemical process.

In Fig. 3(a) is an image of a (La,Ca)O island showing the $\sqrt{2}x\sqrt{2}$ (R45°) pattern of oxygen atoms. The tip was placed in the region marked by the red circle in the figure, and a sawtooth type waveform was applied, with the results shown in the image in Fig. 3(b) and the current trace (as a function of voltage) in Fig. 3(c)[24]. Forward traces are solid lines, reverse traces are dotted lines. The form of the bias waveform is indicated inset in Fig. 3(c). The STM image of the same region after bias application[24], in Fig. 3(b), shows that the application of the bias has resulted in two areas, roughly one atom wide, of dark contrast where previously bright contrast existed (blue circle in Fig. 3(b)). Since we interpret the bright contrast to be oxygen atoms, and the polarity of the waveforms is positive, application of these waveforms is expected to extract oxygen from the lattice at high bias values to give vacancies that appears as regions of dark contrast in the islands. The formation of the two oxygen vacancies in the lattice are correlated with jumps in conductivity as evidenced in the current traces. The first significant event (titled (1) in Fig. 3(c)) is a spike in the current at about 2.2V, while the shorting of the tunnel junction that occurs upon pick-up of the second oxygen atom occurs at about 2.3V. We note here that it is possible that one of the vacancies could have been formed during island reconstruction, with the oxygen moving towards the island edge. Therefore to verify, we confirmed that the experiment is

repeatable, as shown in the before and after STM images in Fig. 3(d,e) and the current trace in Fig. 3(f). A small protrusion to the lower left of the circle in Fig. 3(d), is also no longer existent in Fig. 3(e), and may have been picked up by the tip during the application of the waveform. In this case the current values were much lower, and therefore higher in noise, but the current appears to spike at ~2.3V before immediately dropping to a much lower level of conductivity. A differential image is shown inset in Fig. 3(f) and suggests that there were two vacancies formed here, outlined by the black box.

It is possible to extract semi-quantitative information from the I-V curves. Based on the current spike in Fig. 3(f), the current level reached about -65pA, well above the ~ -20pA that can be extrapolated had the oxygen atom pick-up not occurred. Assuming the exponential dependence of the tunnelling current on tip-sample separation distance i.e. $i \propto e^{-2\kappa\Delta z}$, we can obtain[25] the inverse decay length

$$\kappa = \sqrt{\frac{2m}{\hbar^2}\left(\frac{\phi_t+\phi_s}{2} - E + \frac{e|V|}{2}\right) + k_{\parallel}^2}\,, \qquad (1)$$

through I-Z spectroscopy[24], which gives an average value of $\kappa = 7.449x10^9 m^{-1}$. Substituting I_2/I_1 to find Δz gives Δz~ 79pm change in the height of the tunnelling barrier in this instance. Note that due to instrument smoothing and integration time, current spikes may be larger, so this can be thought of as a lower bound. The same calculation for event (1) in Fig. 3(c) yields ~104pm also, and ~79pm for event (2). However, we note that the spike in the current trace, or the onset of hysteresis, if observed, always appears to occur at ~2.1± 0.17V (95% confidence)[24]. Given the prevalence of the current spike, we surmise that the most likely scenario occurring is that:

(1) Upon application of a critical positive bias V_c, an oxygen from the (La,Ca)O-terminated lattice is removed, and shorts the tunnel junction by moving towards the tip.

(2) This results in a dramatic increase in the measured current due to a reduced tunnelling gap.

(3) The oxygen atom is either ejected due to some instability, or joins the end of the tip-cluster, leaving behind a vacancy in the (La,Ca)O-terminated lattice.

Additionally, we have found that the results of the tip-induced experiments cannot be predicted *apriori*. For example, in Fig. 4(a,b), the same waveform applied to the tip caused a pick-up of a particle, similar to the oxygen atoms in the previous cases. A line profile confirms that the height of the particle/cluster is ~200pm. However, when the waveform was applied to an atom on the edge of an island, as shown in Fig. 4(d), the result is the deposition of atoms onto near where the tip was placed, as shown in Fig. 4(e). A line profile, plotted in Fig. 4(f) of the black and red lines in Fig. 4(d,e) is indicative of single atom deposition of height ~100pm, most likely oxygen. Further investigations into the formation of vacancy clusters and preferential ordering are ongoing.

These studies provide information on the fundamental mechanisms of electrochemical reactions at surfaces as relevant to electrocatalysis and memristor operation[26]. Fundamentally the exploration of atomic level electrochemistry at a manganite surface is a primer, but in the future one can envision determining vacancy formation bias as a function of local texture (for example, distance from an island center), and then correlate this to physical or electrical properties through both STM and non-contact Atomic Force Microsocpy techniques. This approach provides a template for studying physical and electrochemical processes at the atomic scale, and allows

greater insight into electronic phenomena[27,28] in the manganese oxides than has been previously possible.

Acknowledgements

This research was sponsored by the Division of Materials Sciences and Engineering, BES, DOE (RKV, AT, SVK). A portion of this research was conducted at and partially supported by (APB) the Center for Nanophase Materials Sciences, which is a DOE Office of Science User Facility. AGG acknowledges fellowship support from the UT/ORNL Bredesen Center for Interdisciplinary Research and Graduate Education. The authors would like to acknowledge fruitful discussions with P. Ganesh and P. Maksymovych.

References

1 J. Orenstein and A. Millis, Science **288**, 468 (2000).
2 N.F. Mott and L. Friedman, Philosophical Magazine **30**, 389 (1974).
3 M.B. Salamon and M. Jaime, Rev. Mod. Phys. **73**, 583 (2001).
4 P. Sharma, S.B. Kim, T. Koo, S. Guha, and S. Cheong, Phys. Rev. B. **71**, 224416 (2005).
5 M. Fäth, S. Freisem, A. Menovsky, Y. Tomioka, J. Aarts, and J. Mydosh, Science **285**, 1540 (1999).
6 A. Biswas, M. Rajeswari, R. Srivastava, T. Venkatesan, R. Greene, Q. Lu, A. De Lozanne, and A. Millis, Phys. Rev. B. **63**, 184424 (2001).
7 C. Sun, R. Hui, and J. Roller, J Solid State Electrochem **14**, 1125 (2010).
8 C. Moreno, C. Munuera, S. Valencia, F. Kronast, X. Obradors, and C. Ocal, Nano Lett. **10**, 3828 (2010).
9 A. Sawa, Materials today **11**, 28 (2008).
10 S. Piskunov, E. Heifets, T. Jacob, E.A. Kotomin, D.E. Ellis, and E. Spohr, Phys. Rev. B. **78**, 121406 (2008).
11 K. Fuchigami, Z. Gai, T.Z. Ward, L. Yin, P.C. Snijders, E.W. Plummer, and J. Shen, Phys. Rev. Lett. **102**, 066104 (2009).
12 J. Burgy, A. Moreo, and E. Dagotto, Phys. Rev. Lett. **92**, 097202 (2004).
13 C. Renner, G. Aeppli, B.-G. Kim, Y.-A. Soh, and S.-W. Cheong, Nature **416**, 518 (2002).
14 T. Becker, C. Streng, Y. Luo, V. Moshnyaga, B. Damaschke, N. Shannon, and K. Samwer, Phys. Rev. Lett. **89**, 237203 (2002).
15 F. Tsui, M.C. Smoak, T.K. Nath, and C.B. Eom, Appl. Phys. Lett. **76**, 2421 (2000).
16 K. Dörr, O. Bilani-Zeneli, A. Herklotz, A.D. Rata, K. Boldyreva, J.W. Kim, M.C. Dekker, K. Nenkov, L. Schultz, and M. Reibold, Eur. Phys. J. B **71**, 361 (2009).

17 K.H. Ahn, T. Lookman, and A.R. Bishop, Nature **428**, 401 (2004).
18 A. Barnabé, M. Hervieu, C. Martin, A. Maignan, and B. Raveau, J. Appl. Phys. **84**, 5506 (1998).
19 M. Rajeswari, R. Shreekala, A. Goyal, S. Lofland, S. Bhagat, K. Ghosh, R. Sharma, R. Greene, R. Ramesh, and T. Venkatesan, Appl. Phys. Lett. **73**, 2672 (1998).
20 J. Ma, D. Gillaspie, E. Plummer, and J. Shen, Phys. Rev. Lett. **95**, 237210 (2005).
21 A. Tselev, R.K. Vasudevan, A.G. Gianfrancesco, L. Qiao, P. Ganesh, T.L. Meyer, H.N. Lee, M.D. Biegalski, A.P. Baddorf, and S.V. Kalinin, ACS Nano, DOI: 10.1021/acsnano.5b00743 (2015).
22 E. Strelcov, Y. Kim, S. Jesse, Y. Cao, I.N. Ivanov, I.I. Kravchenko, C.-H. Wang, Y.-C. Teng, L.-Q. Chen, Y.H. Chu, and S.V. Kalinin, Nano Lett. **13**, 3455 (2013).
23 R.K. Vasudevan, Y. Liu, J. Li, W.-I. Liang, A. Kumar, S. Jesse, Y.-C. Chen, Y.-H. Chu, V. Nagarajan, and S.V. Kalinin, Nano Lett. **11**, 3346 (2011).
24 See supplemental material at [URL will be inserted by AIP] for supporting information
25 R. de Vries, A. Saedi, D. Kockmann, A. van Houselt, B. Poelsema, and H. Zandvliet, Appl. Phys. Lett. **92**, 174101 (2008).
26 T. Hasegawa, K. Terabe, T. Tsuruoka, and M. Aono, Adv. Mater. **24**, 252 (2012).
27 H. Rønnow, C. Renner, G. Aeppli, T. Kimura, and Y. Tokura, Nature **440**, 1025 (2006).
28 F. Massee, S. de Jong, Y. Huang, W. Siu, I. Santoso, A. Mans, A. Boothroyd, D. Prabhakaran, R. Follath, and A. Varykhalov, Nat. Phys. **7**, 978 (2011).

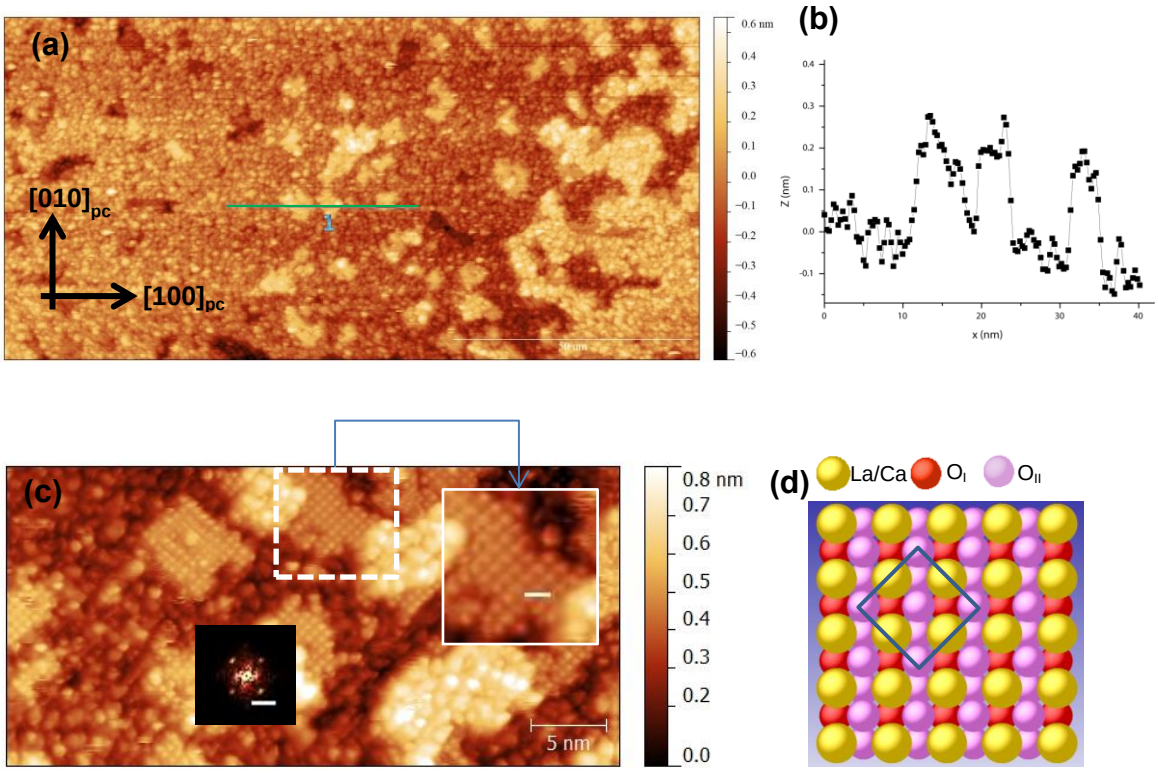

Figure 1: Structure of the film and manganite surface. (a) A typical large-scale STM image of a 24 unit cell thick film. The film grows in an island type growth mode. A line profile of the green line in (a), showing island heights which vary between 200-300pm, roughly half a unit cell is shown in **(b)**. Thus, initially both A ((LaCa)O) and B (MnO_2) terminations are exposed **(c)** A close up scan reveals that the small islands display an ordered lattice with a $(\sqrt{2}x\sqrt{2})R45°$ reconstruction while the other termination appears disordered in the image. An expanded view of the island outlined by the white dotted rectangle is inset, and the FFT of this region is shown below. Scale bar for FFT is $2nm^{-1}$ and scale bar for inset image is 1 nm. **(d)** A schematic of the unreconstructed (La,Ca)O-terminated surface, in a top-down view.

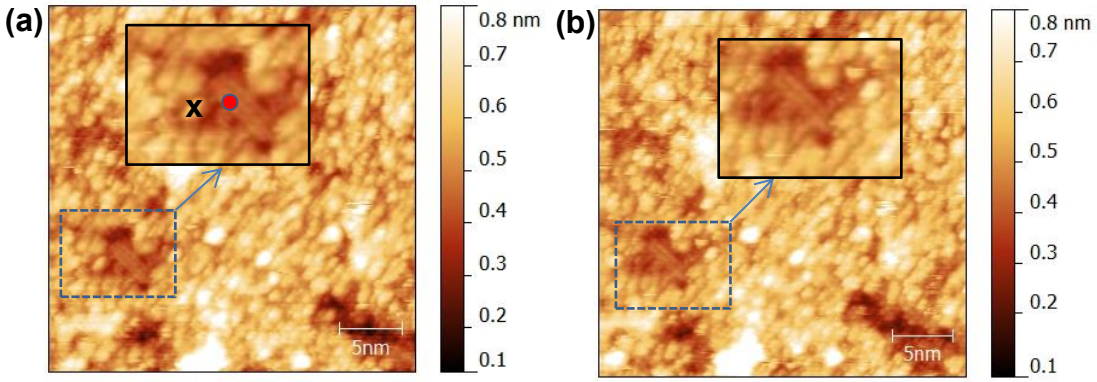

Figure 2: Example of manipulation of the surface by STM. (a) STM image of the surface before manipulation. An expanded view of the region outlined by the blue dashed box is inset. The tip was placed within this island (red circle indicates tip position) and held at +2.5V, with Z-feedback off, for 8s. (b) STM image of the same area after the positive bias application, with the same region expanded.

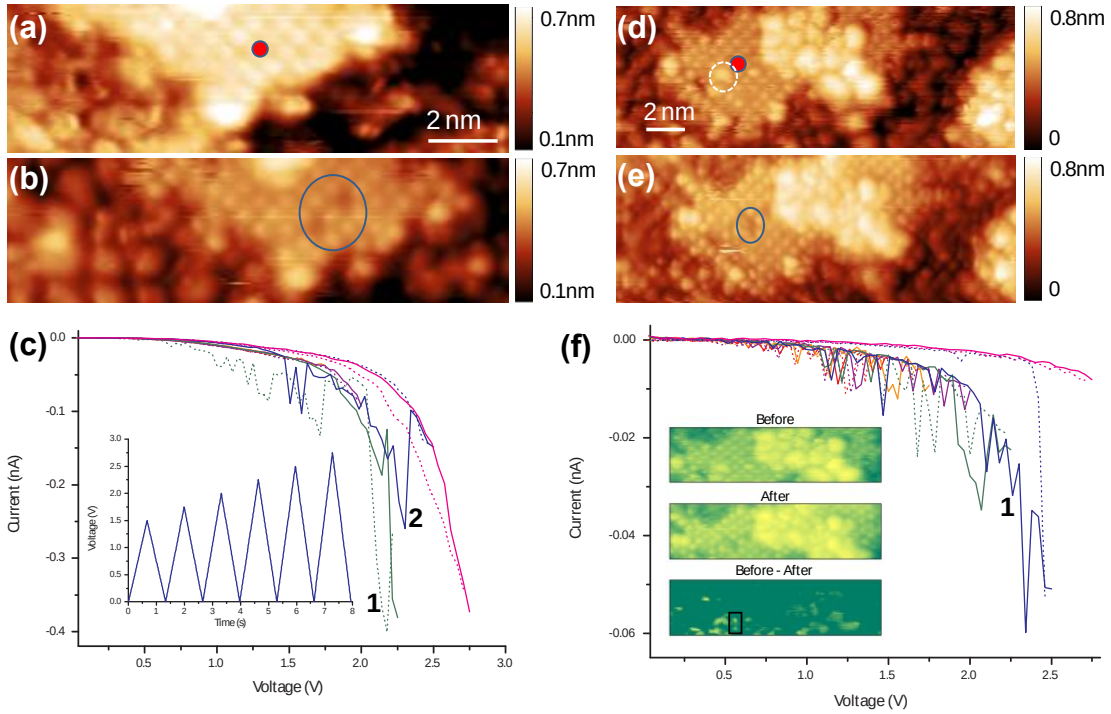

Figure 3: In-situ monitoring of vacancy formation. STM images **(a)** before and **(b)** after a bias waveform was applied to the tip, held at the position indicated by the red circle in (a). The current recorded during this experiment is shown in **(c)** with the bias waveform inset. In this current trace, two large spikes or loop opening features can be easily discerned, and are numbered. These are likely correlated with the formation of the vacancies. Another example of this vacancy formation is shown in the before and after images in **(d)** and **(e)**, respectively. The vacancies formed are outlined by blue circles in (b,e). In addition, it is evident that the protrusion in (d), (white dashed circle), most likely an oxygen adatom, has disappeared in (e). The current trace in **(f)** indicates just one large spike. A differential image is inset, and indicates that two vacancies were formed (bright spots outlined by a black box). Note that in Fig. 3(c,f) the forward part of the current trace is plotted as a solid line, while the reverse part is dotted.

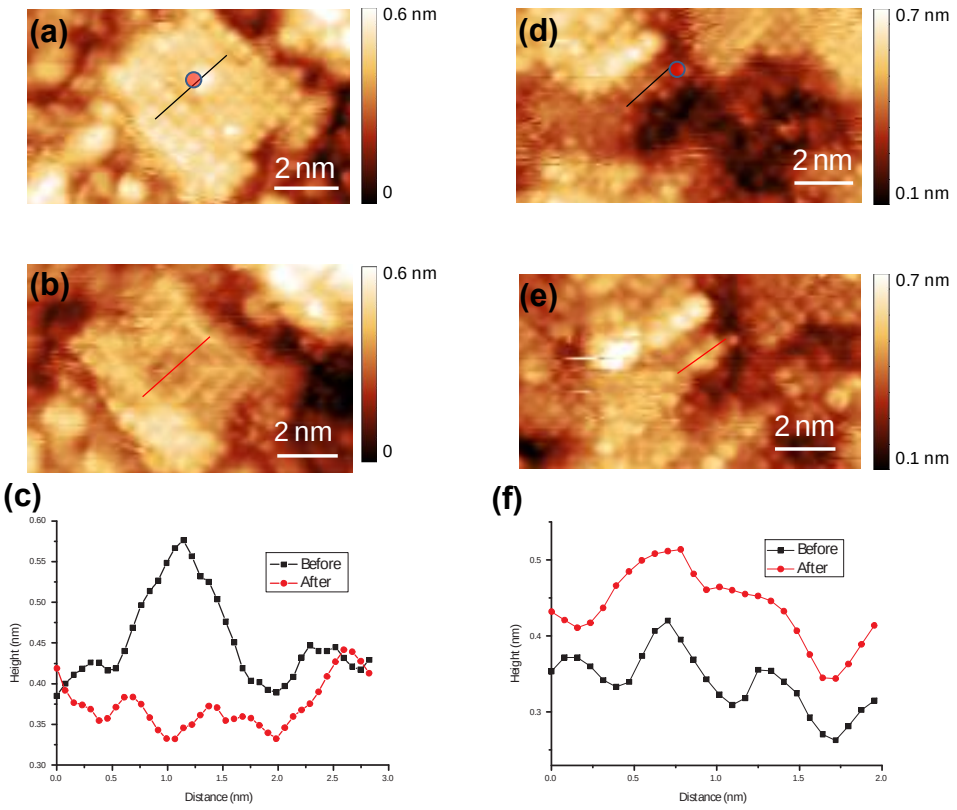

Figure 4: Voltage-induced electrochemistry. STM images taken **(a)** before and **(b)** after the waveform was applied to a particle on the LCO lattice. The position where the tip was placed and the bias waveform was applied is indicated by the red circle in (a). Before and after line profiles from the black and red lines in (a,b) are shown in **(c)**. In **(d)**, the tip was placed on top of the surface on the indicated region (red circle) and the bias waveform was applied. The result is shown in **(e)**, and indicates that at least two atoms have been deposited on top of the original island. Line profiles of the black and red lines in (d,e) are shown in (f), and clearly indicate that the height has increased by ~100pm, consistent with deposition of oxygen atoms.